PHYSICAL REVIEW E **74**, 020401(R) (2006)

Solvophobic solvation at large and intermediate length scales: Size, shape, and solvent effects

Yong Qin and Kristen A. Fichthorn*

Department of Chemical Engineering, The Pennsylvania State University, University Park, Pennsylvania 16802, USA

(Received 19 May 2006; revised manuscript received 17 July 2006; published 22 August 2006)

We report the results of molecular-dynamics simulations of solvophobic nanoparticles in *n*-decane solvent. We observe that solvent ordering in the interparticle gap and solvation forces depend on the particle size and shape. Analogous to hydrophobic hydration, we observe dewetting of the interparticle region when the nanoparticle separation becomes smaller than a critical value of δ_c. We observe that δ_c exhibits a nonmonotonic dependence on nanoparticle size, in contrast to what is expected from studies of water. While studies of hydrophobic hydration indicate that two solute length scales govern hydrophobic interactions, our studies indicate that a third length scale can be important in the more general phenomenon of solvophobic solvation.

DOI: 10.1103/PhysRevE.74.020401 PACS number(s): 82.70.Uv, 82.70.Dd, 83.80.Hj

The interactions between hydrophobic solutes in aqueous solutions have been studied extensively in the areas of dewetting, nanobubble nucleation, protein assembly, and protein folding. A central idea is that water is attracted less strongly to the surfaces of nonpolar solutes in aqueous suspensions than it is to itself [1]. This can lead to a depletion of water around the surfaces of sufficiently large solutes and dewetting of the gap region between the solutes if they come closer than a critical distance of δ_c [2,3]. For sufficiently large solutes, δ_c occurs at a separation when the favorable bulk free energy of water in the gap balances the unfavorable surface energy and can be estimated by [2–4]

$$\delta_c \propto \frac{2\gamma}{\rho|\mu_l - \mu_g|}, \tag{1}$$

where γ is the surface tension, ρ is the bulk density, and μ_l and μ_g are the liquid and vapor chemical potentials, respectively. The pressure imbalance associated with dewetting leads to solute attraction.

Unlike the larger hydrophobes, solutes such as argon and methane are too small to perturb the hydrogen-bonding network of water. When such small solutes are brought close together, dewetting does not occur and solvent interactions may disfavor their aggregation [5–8]. The transition between "small" and "large" solutes has been predicted theoretically [2] and studied with computer simulations [3,7–9]. The complex, multiscale nature of these interactions is believed to come into play in protein folding and assembly [10–12] where a wide range of length scales is present.

Although hydrophobic hydration has been extensively studied, this is just a specialized case of the more general phenomenon of "solvophobic solvation," which can occur in a wide variety of applications involving solutes in nonaqueous solutions, including colloid and polymer suspensions and assemblies. In this paper, we show that the more general phenomenon of solvophobic solvation can exhibit many features associated with its aqueous counterpart, although there are some important differences. In particular, we demonstrate that solvent ordering at the solvent-solute interface can depend on both the size and shape of nanoparticle solutes, leading to complex and varied nanoparticle-nanoparticle force profiles. We find that the nanoparticle size dependence of solvent ordering leads to a delineation of the "large" solute-size regime for hydrophobic hydration into "intermediate" and "large" length scales in the general scenario of solvophobic solvation. The existence of three solute size regimes provides greater flexibility for creating hierarchical, nonaqueous assemblies involving polymers and nanoparticles.

We use parallel molecular-dynamics (MD) simulations to probe two solvophobic nanoparticles immersed in an *n*-decane ($C_{10}H_{22}$) liquid. The decane molecules are simulated using the united-atom (UA) model [13]. In the UA model, each methyl ($-CH_3$) and methylene ($-CH_2-$) group is treated as a single UA with the center residing on the carbon atom. The C-C bond length is constrained with the RATTLE algorithm [14]. A truncated Lennard-Jones (LJ) 12-6 potential is utilized to calculate the intermolecular interactions between UAs and atoms in the nanoparticles. To model the solvophobic effect, the UA-solid atom interaction is 1/5 of the UA-UA intermolecular interaction ($\varepsilon_{sl}=1/5\varepsilon_{ll}$). For some of the simulations, we used $\varepsilon_{sl}=1/2\varepsilon_{ll}$ and we found that this changes the magnitude of the interparticle forces without qualitatively changing the force profile. The nanoparticles are modeled as rigid and immobile clusters of atoms. Two types of nanoparticles with different sizes and shapes are considered. Two of the nanoparticles are rough, amorphous spheres formed by simulated condensation of a LJ liquid. The small sphere is composed of 64 LJ atoms and has an average diameter of 4.9σ. The end-to-end length of an all-*trans* *n*-decane molecule ($L\approx 3.3\sigma$) is comparable to the diameter of the small sphere. The large sphere is composed of 2048 LJ atoms, and the average diameter is 17.6σ. In addition to the spheres, we studied small ($7\times7\times7$) and large ($14\times14\times14$) fcc cubes, oriented so that their contacting surfaces have the fcc(111) structure. The side of a cube face is 6.6σ and 13.2σ in length for the small and large cubes, respectively.

The simulations are carried out in the *NVT* ensemble, with the temperature fixed at $T=293.15$ K and a liquid density of $\rho=0.73$ g/mL, or a dimensionless segment density of

*Electronic address: fichthorn@psu.edu; also at the Department of Physics, Pennsylvania State University, University Park, PA 16802.

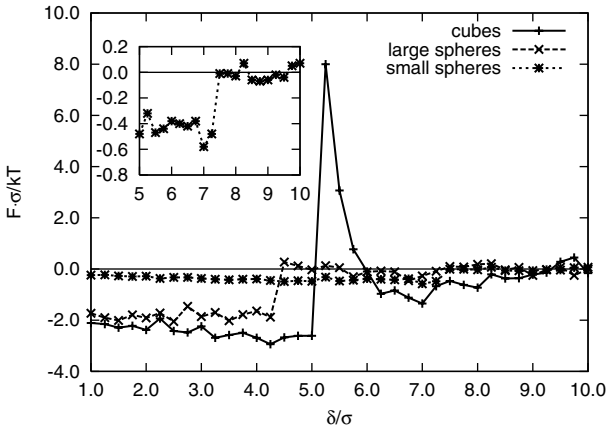

FIG. 1. Solvophobic solvation forces as a function of nanoparticle separation δ. Solvation forces jump at 5.25σ, 4.50σ, and 7.50σ for large cubes, large spheres, and small spheres, respectively. Not shown (for clarity) is the force profile of the small cube, which exhibits qualitatively the same features with a jump at 8.5σ. The inset shows the force profile near δ_c for the small spheres.

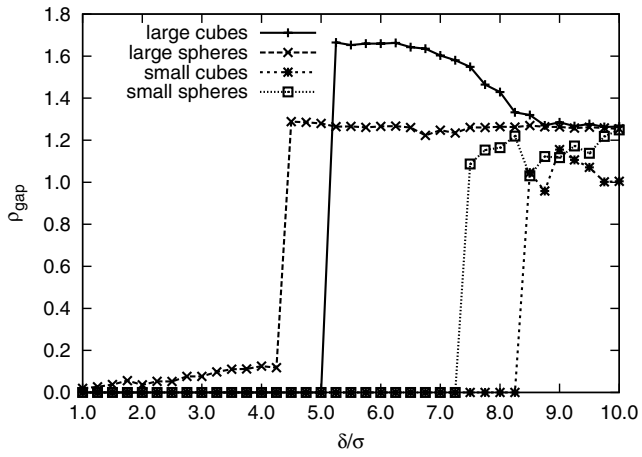

FIG. 2. The average density profiles of *n*-decane in the interparticle gap as a function of separation δ.

$1.2\sigma^{-3}$. For simulations of the large cubes, we varied the box dimensions to maintain a constant liquid density sufficiently far from the cube surfaces at various cube separations and we found that the results are insensitive to small variations in the bulk density. Depending on the size of nanoparticles, between 3046 and 10 794 decane solvent molecules are simulated. We obtain the solvation force $\hat{F}^S$ as a function of nanoparticle separation δ using

$$\hat{F}^S(\delta) = \langle \hat{r}_{AB} \cdot (\hat{F}_{AF} - \hat{F}_{BF}) \rangle_\delta, \tag{2}$$

in which $\hat{F}_{AF}(\delta)$ and $\hat{F}_{BF}(\delta)$ are the fluid forces on particles A and B and $\hat{r}_{AB}$ is the unit vector pointing from the center of mass of A to that of B. Here, δ is defined as the distance along $\hat{r}_{AB}$ between the closest two atoms in the different nanoparticles. Since the nanoparticles are immobile, there is a one-to-one correspondence between δ and the nanoparticle center-of-mass separation. The nanoparticles are first equilibrated for more than 2 ns at a separation of 10σ. Subsequent to this, solvation forces are obtained as ensemble averages in production runs ranging from 0.4 (large nanoparticles) to 2 (small nanoparticles) ns in duration. The first production run occurs for nanoparticles at the separation of 10σ, then the separation is decreased by 0.25σ, there is another equilibration, and solvation forces are obtained in another production run. This procedure is repeated until the nanoparticle separation is 1.0σ. Additionally, we tested for hysteresis by executing production runs in which the nanoparticle separation was increased at certain critical distances. No hysteresis was observed.

Figure 1 shows the solvation-force profiles obtained for three of the nanoparticle systems. While there are individual variations, all exhibit a discontinuous jump to attraction at a critical separation of δ_c. Discontinuous jumps in the solvation forces have been observed in simulation studies of LJ liquids near solvophobic surfaces at sufficiently low temperatures [15] and for water confined between hydrophobic surfaces [16,17]. In these studies, hysteresis was observed near the jumping point. We did not observe hysteresis here, which may be attributed to the temperature probed or a small free-energy barrier for nucleating a nanobubble in the interparticle gap.

We are able to correlate the discontinuous jumps in the solvation-force profiles with dewetting of solvent from the interparticle gap. Figure 2 shows the segment density in the interparticle gap ρ_{gap} as a function of nanoparticle separation. The gap densities are initially obtained as the number of UAs in the gap volume V_{gap}. We obtain the gap volume using $V_{\text{gap}} = \pi d^2 l_c/4 - \pi d^3/6$ for spheres and $V_{\text{gap}} = A\delta$ for cubes, where d is the sphere diameter, l_c is the center-of-mass separation between two nanoparticles, and A is the area of a cube face. We then update this initial estimate by taking into account the presence of a thin depletion layer of thickness w surrounding the nanoparticle surfaces, as discussed below. Comparing Figs. 1 and 2, we see that the force and density jumps occur at exactly the same separations for all the objects.

Although the attractive force jumps are directly linked to dewetting, other features of the force profile correlate with solvent ordering in the gap. For example, as the cubic nanoparticles approach one another, decane molecules in the interparticle gap undergo an ordering transition from a disordered, liquidlike structure to a highly ordered, solidlike structure, which culminates at the critical separation of $\delta_c \cong 5.25\sigma$. Figure 3 shows this ordered structure at δ_c, where we see that the decane molecules orient themselves perpendicular to the solid surfaces in a single layer. These molecules have a small tilt angle of their end-to-end vector with respect to the surface normal ($<10°$), and their propensity to assume the all-*trans* conformation is greater than that of bulk liquid decane (97% versus 72% in the bulk). In this way, *n*-decane molecules maximize their self-interaction, while minimizing their contact with the surface. Concomitant with the ordering of confined decane is a repulsive increase in the solvation force.

Solidlike ordering and associated repulsive solvation forces have been observed in computer-simulation studies of *n*-alkanes in the surface forces apparatus (SFA) [18–20],

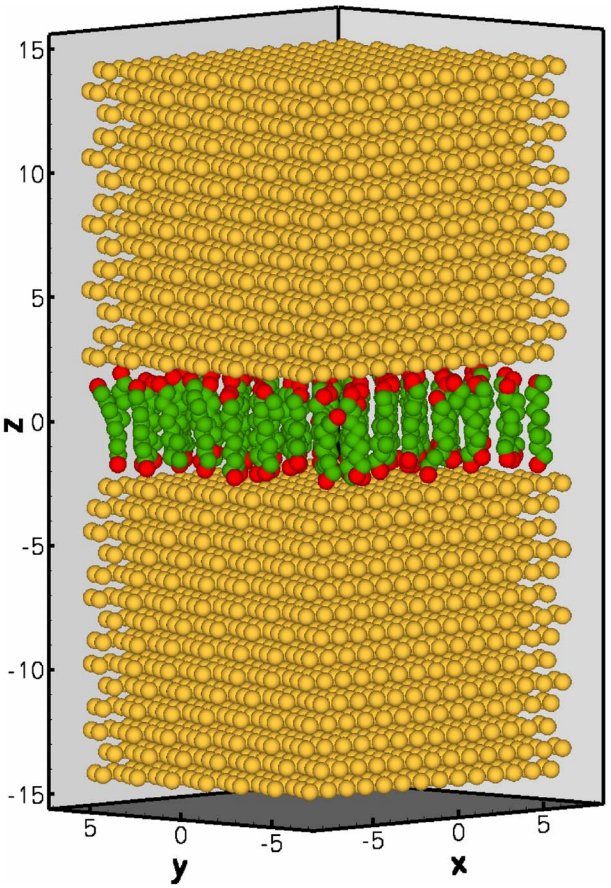

FIG. 3. (Color online) A snapshot of *n*-decane molecules confined between two solvophobic nanocubes at a separation of $\delta_c = 5.25\sigma$. The methyl end groups of decane are red (dark) and the methylene groups are green (light).

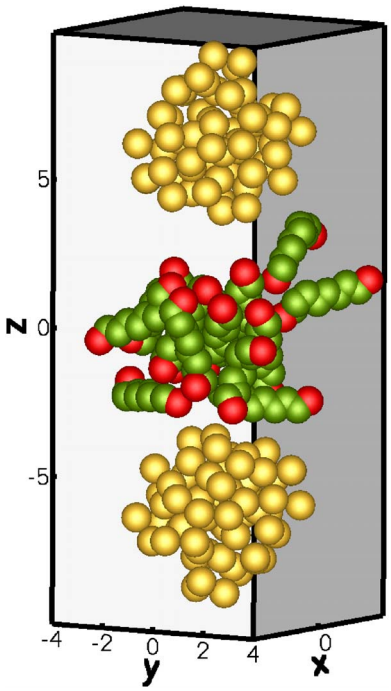

FIG. 4. (Color online) A snapshot of *n*-decane molecules confined between the small spheres at the critical separation of $\delta_c = 7.5\sigma$. Shown are decane molecules that have at least one of their UAs in the interparticle gap.

although the confining surfaces in these studies were "solvophilic" instead of the "solvophobic" surfaces considered here. We observed that decane molecules also tend to orient themselves normal to the surfaces of the spheres and the small cubes. However, due to the roughness and curvature of the spheres, the ordering is not nearly as pronounced as it is for the large cubes and no repulsion occurs in their solvation forces. These findings are in agreement with experimental studies of with the SFA [21–23] and computer simulations [24–26], which indicate that surface roughness reduces solvent ordering and solvation forces for *macroscopic* surfaces. Interestingly, we did not observe strong decane ordering in the interparticle gap between the small cubes. We will return to this point below.

It is of interest to understand the structure of *n*-decane near its interface with the nanoparticles. As expected from studies of water [2,27], we observe a thin, vaporlike depletion layer of width w around the nanoparticle surfaces. An example of this layer can be seen in Fig. 4. We estimated w for the large nanoparticles by calculating solvent gap densities (cf. Fig. 2). If w is zero, then the gap density has its minimum value. The gap density increases with increasing w until a constant value is attained. We found that the incipient value for a constant w depends on the nanoparticle shape and separation: For the large cubes near δ_c, where the confined fluid has a solidlike structure, w can be as small as 0.9σ, whereas for the large spheres and cubes with larger separations, a more disordered decane structure occurs in the gap and w has a larger value of 2.2σ.

We observe that liquid decane assumes a significantly different structure at the depletion-layer interface than it does at its liquid-vapor interface. In MD simulation studies, it has been observed that *n*-decane molecules at the liquid-vapor interface orient themselves with their long axis parallel to the interface and that there is a perpendicular layer of molecules underneath them [28]. In our study, the perpendicular interfacial *n*-decane molecules near the surfaces of the large cubes and spheres have a qualitatively similar structure to that observed experimentally for surface freezing at the liquid-vapor interface of longer *n*-alkanes [29]. Thus, the interfacial structures of decane observed for the large nanoparticles are consistent with confinement-induced freezing.

It is interesting to consider the origins of the disparate jumping points in Figs. 1 and 2. Following the macroscopic arguments suggested by Eq. (1), we expect dewetting to occur at a critical separation that is proportional to the ratio of the gap volume V_{gap} to the area of the solid surfaces bounding the gap A_{gap}, i.e., $\delta_c \propto (V_{\mathrm{gap}}/A_{\mathrm{gap}})_c$. Such macroscopic arguments can be successfully applied to the large spheres and the cubes, which both dewet at $(V_{\mathrm{gap}}/A_{\mathrm{gap}})_c \cong 2.5\sigma$. However, the small spheres and cubes exhibit a greater δ_c than the large nanoparticles. These results are counterintuitive based on knowledge from studies of water, which indicate that δ_c decreases to zero as the solute size decreases [2,3].

Some insight into these differences can be gained from Fig. 4, which shows the small spheres and all the decane molecules that have at least one segment in the interparticle gap at δ_c. We observe qualitatively similar results for the small cubes. In this snapshot, there are only six decane molecules that reside entirely in the gap region. Although this number fluctuates over time, typically fewer than ten molecules reside entirely in the gap for the small spheres. Thus, even though the small spheres in Fig. 4 have a greater separation than the large cubes in Fig. 3, the gap volume is considerably smaller—especially considering the size constraints of a molecule as large as decane. While decane is able to achieve ordered structures in the gaps between the larger nanoparticles (cf. Fig. 3), which provide a high cohesive energy density in the gap region, ordering is difficult for molecules in the interparticle gap between the small nanoparticles. Figure 4 reveals that a significant number of molecules lie at the gap-bulk interface, with some of their segments in the gap and some in the bulk. Molecular ordering is frustrated by this gap-bulk interface. As a result, the cohesive energy density is weakened, it cannot overcome the unfavorable interfacial energy, and the nanoparticles jump together.

There are important differences between the solvophobic dewetting transitions that we observe here and hydrophobic dewetting. If we consider key attributes of the interparticle gap and its solvophobic collapse, we note that the small nanoparticles studied here possess qualitative attributes associated with the hydrophobic collapse of large hydrophobes. The *n*-decane molecules in the gap between small nanoparticles in the 1–2 nm size regime retain a disordered, liquidlike structure that persists until a separation at which nearly every molecule resides at a gap interface and solvophobic collapse occurs. The large spheres and cubes in the 5–6 nm regime, however, exhibit a different scenario from that expected for the hydrophobic collapse of large hydrophobes. When confined between the extended surfaces of these larger objects, *n*-decane molecules are able to order into structures that are significantly different from the bulk. These structures provide a high cohesive energy density and they stabilize the interparticle gap so that the larger nanoparticles are able to come closer together than the small ones. This "intermediate" to "large" transition is not anticipated in theories of hydrophobic hydration, but it could occur in the more general scenario of solvophobic solvation.

This work was funded by an EPA Star Grant program, Grant No. R-8290501, the Petroleum Research Fund of the American Chemical Society, and the NSF, Grant No. CCR-0303976.

[1] D. Chandler, Nature (London) **417**, 491 (2002).
[2] K. Lum, D. Chandler, and J. D. Weeks, J. Phys. Chem. B **103**, 4570 (1999).
[3] X. Huang, C. J. Margulis, and B. J. Berne, Proc. Natl. Acad. Sci. U.S.A. **100**, 11953 (2003).
[4] K. Lum and A. Luzar, Phys. Rev. E **56**, R6283 (1997).
[5] L. R. Pratt and D. Chandler, J. Chem. Phys. **67**, 3683 (1977).
[6] C. Pangali, M. Rao, and B. J. Berne, J. Chem. Phys. **71**, 2975 (1979).
[7] X. Huang, C. J. Margulis, and B. J. Berne, J. Phys. Chem. B **107**, 11742 (2003).
[8] N. Choudhury and B. M. Pettitt, J. Am. Chem. Soc. **127**, 3556 (2005).
[9] S. Rajamani, T. M. Truskett, and S. Garde, Proc. Natl. Acad. Sci. U.S.A. **102**, 9475 (2005).
[10] K. A. Dill, Biochemistry **29**, 7133 (1990).
[11] D. M. Huang and D. Chandler, Proc. Natl. Acad. Sci. U.S.A. **97**, 8324 (2000).
[12] R. Zhou, X. Huang, C. J. Margulis, and B. J. Berne, Science **305**, 1605 (2004).
[13] J. P. Ryckaert and A. Bellemans, Faraday Discuss. Chem. Soc. **66**, 95 (1978).
[14] H. C. Andersen, J. Comput. Phys. **52**, 24 (1983).
[15] P. G. Bolhuis and D. Chandler, J. Chem. Phys. **113**, 8154 (2000).
[16] A. Wallqvist and B. J. Berne, J. Phys. Chem. **99**, 2893 (1995).
[17] T. Koishi *et al.*, Phys. Rev. Lett. **93**, 185701 (2004).
[18] J. Gao, W. D. Luedtke, and U. Landman, J. Chem. Phys. **106**, 4309 (1997).
[19] F. Porcheron, B. Rousseau, M. Schoen, and A. H. Fuchs, Phys. Chem. Chem. Phys. **2**, 1115 (2001).
[20] J.-C. Wang and K. A. Fichthorn, J. Chem. Phys. **116**, 410 (2002).
[21] H. K. Christenson, J. Phys. Chem. **90**, 4 (1986).
[22] M. Heuberger and M. Zäch, Langmuir **19**, 1943 (2003).
[23] Y. Zhu and S. Granick, Langmuir **19**, 8148 (2003).
[24] L. J. D. Frink and F. van Swol, J. Chem. Phys. **108**, 5588 (1998).
[25] J. P. Gao, W. D. Luedtke, and U. Landman, Tribol. Lett. **9**, 3 (2000).
[26] C. Ghatak and K. G. Ayappa, J. Chem. Phys. **120**, 9703 (2004).
[27] F. H. Stillinger, J. Solution Chem. **2**, 141 (1973).
[28] J. G. Harris, J. Phys. Chem. **96**, 5077 (1992).
[29] X. Z. Wu, E. B. Sirota, S. K. Sinha, B. M. Ocko, and M. Deutsch, Phys. Rev. Lett. **70**, 958 (1992).